

In₂ZrBr₆: A Van Vleck-Type Paramagnetism by Indirect Coupling

Richard Dronskowski

Contribution from the Max-Planck-Institut für Festkörperforschung, Heisenbergstrasse 1, 70 569 Stuttgart, Germany

Received August 15, 1994[⊗]

Abstract: Tetragonal In₂ZrBr₆, a slightly distorted variant of the K₂PtCl₆ structure type, contains almost cuboctahedral InBr₁₂¹¹⁻ units that are sharing trigonal faces with ZrBr₆²⁻ complex anions. In₂ZrBr₆ is a weak van Vleck-type paramagnet, and we propose that this behavior originates from an indirect electronic coupling between occupied bands with strong indium 5s character and unoccupied, fairly localized zirconium 4d crystal orbitals, moderated by bridging Br⁻ anions. In⁺ is weakly and nondirectionally bonded to coordinating Br⁻ (there is an almost insignificant indium 5p bonding contribution) and the crystal potential around In⁺ turns out to be very soft because of antibonding In⁺–Br⁻ interactions within the highest occupied bands.

1. Introduction

The crystal structures of the reduced binary indium bromides have been clarified not too long ago by Staffel and Meyer, by Beck, and by Bärnighausen.^{1–4} Probably the most striking feature of these structures is the appearance of fairly uncommon, strongly distorted coordination polyhedra around the univalent indium cations (7- to 10-fold coordination). Self-consistent calculations of the electronic structures of these materials⁵ explain this phenomenon by referring to *antibonding* In⁺–Br⁻ interactions within the highest occupied bands that have mostly indium 5s character. All coordination polyhedra reported so far are almost equally well optimized with respect to In⁺–Br⁻ bond strengths. Also, there is a delicate balance between the volume chemistry (space requirement) of In⁺ on one side and the repulsive Br⁻–Br⁻ interactions on the other which have to be minimized. There is no influence, however, of a *directed* electron “lone-pair” influencing coordination polyhedron geometry in any of the structures studied.

2. Synthesis and Structure

The discovery of only weak In⁺–Br⁻ bonding inside the binary compounds, favoring distorted coordination polyhedra, led to the idea of a possible preparation of a new phase containing a highly *symmetric* Br⁻ polyhedron around In⁺. Among several possibilities, the classical K₂PtCl₆ structure type seemed to be promising. On the basis of the hypothetical stoichiometry “In₂ZrBr₆”, a cuboctahedral InBr₁₂¹¹⁻ unit was the goal, hopefully as large as possible through the size-determining influence of the neighboring ZrBr₆²⁻ building block (Zr⁴⁺ is the largest tetravalent transition metal ion).⁶

Indeed, In₂ZrBr₆ may be synthesized by oxidation of elemental Zr within an InBr₃ melt (4 days at 475 °C), followed by subsequent slow cooling (2 °C/h). The new phase crystallizes as slightly greenish-yellow, transparent little blocks that are extremely sensitive to air and humidity.

The single crystal structure refinement in space group *Fm* $\bar{3}$ *m* ($a \approx 1053$ pm, $z(\text{Br}) = 0.2456(6)$, $R \approx 0.12$, strongly elongated thermal ellipsoids for Br⁻), however, happened to be completely unsatisfactory. Its poor performance can be understood because of the presence of an almost perfectly grown twin individual. As it turns out, Guinier diffractograms of the powder give evidence for some split reflections, allowing only a tetragonal unit cell due to homological criteria;⁷ although it seems to be I-centered at first sight, this is faked by partial occupations of some special Wyckoff positions. A Rietveld refinement on powder data⁸ in a primitive space group (Figure 1), eventually converged to an unexpected high precision (with respect to standard X-ray powder methodology).

The lattice constants were found to be $a = 740.44(4)$ pm and $c = 1069.68(7)$ pm while the refined positions in space group *P4/mnc* (No. 128) are as follows: In in 4d; Zr in 2a; Br(1) in 8h with $x = 0.2836(5)$, $y = 0.2163(4)$; Br(2) in 4e with $z = 0.2454(6)$. The isotropic displacement parameter of indium, using a $B_{\text{In}}:B_{\text{Zr}}:B_{\text{Br}} \equiv 1:0.5:0.8$ constraint, comes to $B = 1.74(3)$ Å². The residual values and the goodness-of-fit (GooF) are $R_p = 0.033$, $R_{\text{wp}} = 0.046$, $R_{\text{Bragg}} = 0.034$, and $\text{GooF} = 1.23$ for 169 Bragg reflections (4501 data points) and 12 refinable parameters.

A [001] projection of the room-temperature structure (or modification) of In₂ZrBr₆ (Figure 2), a tetragonally distorted K₂PtCl₆ structure type variant, shows the small (7.8°) tilt of the ZrBr₆²⁻ octahedra against the 4-fold axis. Besides recently described tellurobromozirconates,⁹ the ZrBr₆²⁻ unit found here surprisingly seems to be the only available crystal-chemical example of a tetravalent Zr bromide. Within the scope of the resolution, the unit shows octahedral symmetry, having Zr⁴⁺–

(7) Mirkin, L. I. *Handbook of X-Ray Analysis of Polycrystalline Materials*; Consultants Bureau: New York, 1964.

(8) The collection of X-ray data was performed at room temperature (20 °C) with a calibrated (silicon standard) STOE Stadi powder diffractometer (sample in 0.3 mm capillary; Cu K α radiation; 2θ scan with $10 \leq 2\theta \leq 100^\circ$ and 0.02° step width). The Rietveld powder refinement was done using program DBW 9006²⁶ and scattering factors of the neutral atoms (Mod 2 Lorentz profile function; one instrument parameter, three parameters for reflection shape (half width), one asymmetry parameter, one overall scale parameter, two parameters for lattice constants, three spatial parameters, one isotropic displacement parameter).

(9) The compounds (Te₄)(Zr₂Br₁₀) and (TeBr₃)(Zr₂Br₉) contain edge-sharing, distorted ZrBr₆²⁻ units; the average Zr⁴⁺–Br⁻ distance is 263.4 pm. Unfortunately, no librational analysis was performed, despite an anisotropic refinement: Beck, J. *Chem. Ber.* **1991**, *124*, 677–681.

[⊗] Abstract published in *Advance ACS Abstracts*, January 15, 1995.

(1) Staffel, T.; Meyer, G. *Z. Anorg. Allg. Chem.* **1987**, *552*, 113–122; **1988**, *563*, 27–37.

(2) Beck, H. P. *Z. Naturforsch.* **1987**, *42B*, 251–252.

(3) Bärnighausen, H. *Z. Kristallogr.* **1989**, *186*, 16–18.

(4) Marsh, R. E.; Meyer, G. *Z. Anorg. Allg. Chem.* **1990**, *582*, 128–130.

(5) Dronskowski, R. *Inorg. Chem.* **1994**, *33*, 6201–6212.

(6) Shannon, R. D. *Acta Crystallogr.* **1976**, *A32*, 751–767.

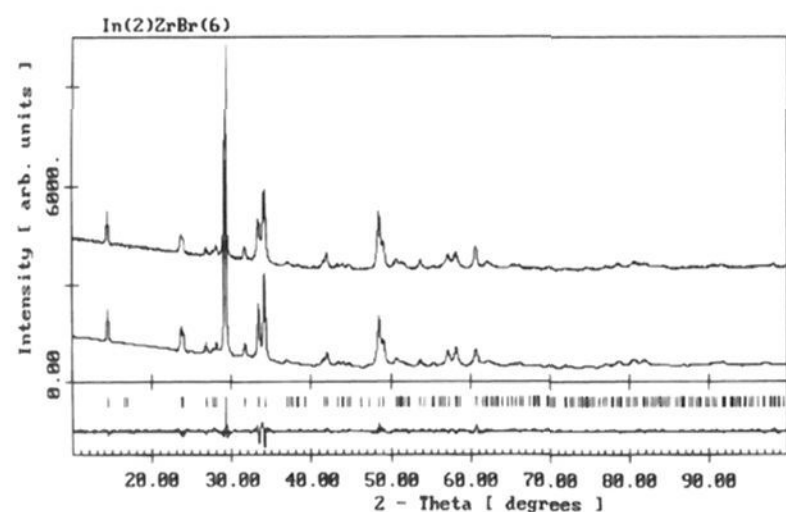


Figure 1. Rietveld refinement of tetragonal In_2ZrBr_6 : depicted are (from top to bottom) measured and fitted diffraction patterns, calculated positions of the Bragg peaks, and the difference between measured and calculated intensities.

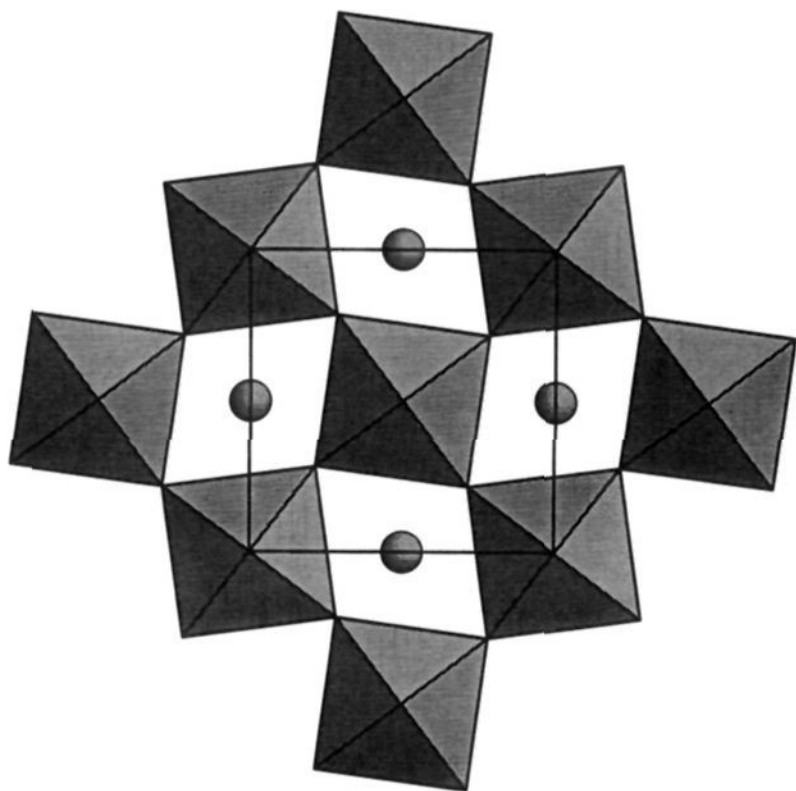


Figure 2. Projection of the crystal structure of tetragonal In_2ZrBr_6 along [001] with shaded ZrBr_6^{2-} octahedra and In^+ ions within the approximately cuboctahedral cavities.

Br^- distances of $2 \times 262.5(7)$ pm (along c) and $4 \times 264.1(4)$ pm (within ab plane). This is about 4 pm shorter than the sum of the effective ionic radii (268 pm);⁶ experience suggests that one may expect a librational analysis of the octahedron to maximally widen the bonds by that amount.

The symmetry of the InBr_{12}^{11-} unit is not cuboctahedral but $222 (D_2)$, and instead of finding 12 identical $\text{In}^+ - \text{Br}^-$ distances of 372.4 pm (cubically averaged structure), there are three groups with significantly different bond lengths (Figure 3). Within a classical interpretation, the empirical bond order sum for In^+ is thus increased from 0.69 (cubically averaged structure) to 0.77.¹⁰ Even a semiempirical, quantum mechanical treatment¹¹ shows that the tetragonal structure is more stable than the cubically averaged one by roughly 77 kJ/mol. However,

(10) This calculation is based on the one-parameter formula of Brown and Altermatt: Brown, I. D.; Altermatt, D. *Acta Crystallogr.* **1985**, *B41*, 244–247. The reference distance r_0 of 266.7 pm has been optimized quite recently.⁵

(11) Three-dimensional band structure calculations were performed using a charge-self-consistent²⁷ extended Hückel Hamiltonian²⁸ and a weighted WH approximation²⁹ (CSC-EH-TB). The Slater-type orbital basis set is from a fit to Herman–Skillman functions for neutral atoms,³⁰ and the iteration parameters were taken from the literature³¹ (In, Zr) or from our own investigations (Br).⁵ The diagonalization was done using 45 (19) k points within the irreducible wedge of the tetragonal (cubic) Brillouin zones with the help of a modified³² EHMACC program.³³

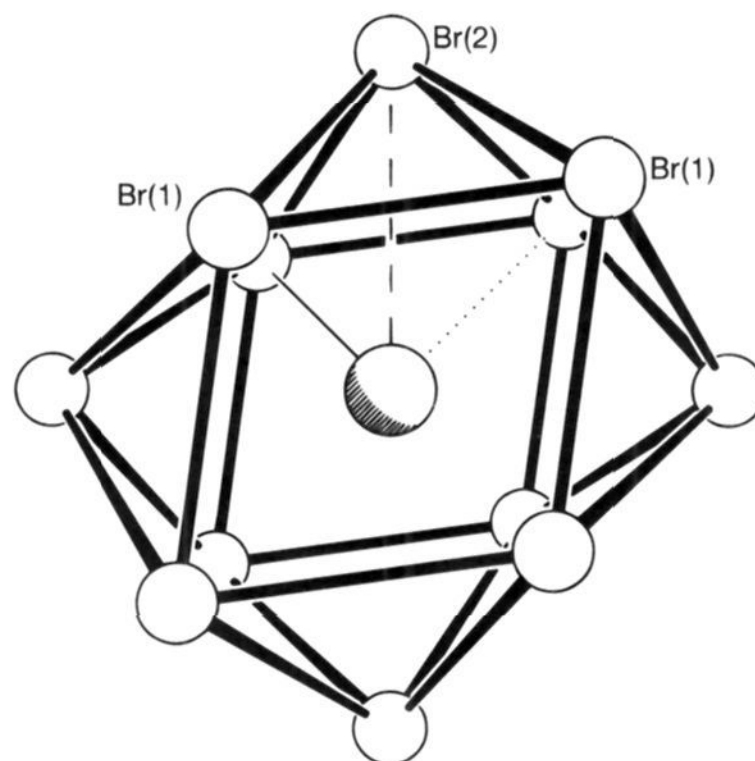


Figure 3. Perspective representation (along [001]) of the tetragonally distorted, almost cuboctahedral InBr_{12}^{11-} unit in the room-temperature modification of In_2ZrBr_6 . In this highest symmetrical $\text{In}^+ - \text{Br}^-$ polyhedron reported so far, In^+ (middle) has the local symmetry $222 (D_2)$, and there are three different $\text{In}^+ - \text{Br}^-$ distances, 350.5(3) pm (solid line), 370.3(1) pm (dashed), and 399.7(3) pm (dotted), each of them occurring four times.

the classical bond length–bond strength reasoning then appears to be incorrect (see below), since $\text{In}^+ - \text{Br}^-$ bond strength differences are *not* responsible for the cubic/tetragonal competition. Surprisingly, the absolute electronic hardness¹² of the tetragonal structure is 1.05 eV, *lowered* by more than 0.3 eV compared to that of the cubically averaged one, a result that has never been found previously for a *more* stable structure. Typically, the greater the stability, the larger the electronic hardness.

Temperature-dependent X-ray powder investigations following the Guinier–Simon technique¹³ prove that the tetragonal room-temperature phase of In_2ZrBr_6 transforms continuously into a cubic structure at elevated temperatures; this process is completed at 172 °C. At 275 °C one finds $a = 1066.49(9)$ pm (10 reflections, $Fm\bar{3}m$).

At lower temperatures, on the other hand, there is a transformation to a primitive monoclinic structure starting at -1 °C, with only tiny deviations away from tetragonal metrics¹⁴ and reflecting a small tilting of the octahedral building blocks against the c axis. Thus, the observed symmetry reduction (cubic \rightarrow tetragonal \rightarrow monoclinic) corresponds to a group–subgroup relationship¹⁵ of the form

$$Fm\bar{3}m \xrightarrow{t_3} (I4/mmm; a' = a\sqrt{2}, c' = a) \xrightarrow{k_2} P4/mnc \xrightarrow{t_2} (Pnmm) \xrightarrow{t_2} P2_1/n$$

(12) The absolute electronic hardness measures the electronic resistance of a quantum system (atom, molecule, crystal) with respect to an external electronic perturbation (attack of a reagent): Parr, R. G.; Pearson, R. G. *J. Am. Chem. Soc.* **1983**, *105*, 7512–7516.

(13) Simon, A. *J. Appl. Crystallogr.* **1970**, *3*, 18–21.

(14) The lattice constants lie approximately around 735, 737, and 1057 pm, and the monoclinic angle is roughly 90.5° (11 reflections, $P2_1/n$). An accurate refinement of the lattice constants, based only on unambiguously indexed Bragg peaks, is strongly underdetermined because of too many overlapping reflections. The overall trend of the lattice constants as well as the nearly 2% contraction of the cell volume, however, are very reasonable.

(15) Bärnighausen, H. *Comm. Math. Chem.* **1980**, *9*, 139–175.

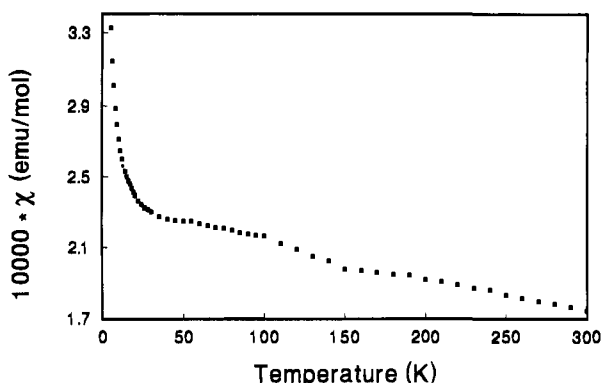


Figure 4. Molar susceptibility as a function of temperature for In_2ZrBr_6 ($H = 1$ T). The data were first corrected with respect to diamagnetic shielding of the ionic cores.⁴¹ The increase in molar susceptibility below 30 K is probably due to paramagnetic pollutants.

Transformations of this kind have already been reported by Abriel for the case of alkali halide tellurates,^{16,17} and there are hints of similar transformations in a stannate¹⁸ and in platinates.¹⁹ The origins of these structural changes (see below) remain to be uncovered.

3. Physical and Electronic Properties

3.1. Magnetism and Chemical Bonding. For In_2ZrBr_6 , there is an astonishing observation of an (approximately) temperature-independent paramagnetism (TIP) of seemingly van Vleck-type (Figure 4). This phenomenon should be due to an unusual electronic configuration of In_2ZrBr_6 which, according to van Vleck's original definition,²⁰ is characterized from a mixing between the nonmagnetic electronic ground state and higher, unoccupied states that have a nonvanishing angular momentum, l , in other words, with some p, d, or f character. Such a paramagnetic susceptibility contribution would then be expressed as

$$\chi = \frac{2}{3} N_A \sum_{n \neq 0} \frac{|\mathbf{m}^0(0;n)|^2}{E(0;n)}$$

where $\mathbf{m}^0(0;n)$ is the matrix element of the orbital angular momentum operator for an electron that is promoted from the ground state into the n th excited state. $E(0;n)$ is the corresponding excitation energy and N_A is Avogadro's number.

In order to elucidate the magnetic mechanism, a theoretical density-of-states (depicted in Figure 5) was calculated on a semiempirical level, its numerical details coinciding almost quantitatively with likewise performed *ab initio* calculations (see below) in all points. For example, one finds roughly the same relative positions for H_{ii} values (one-electron approximation) and band centers C (many-particle theory) and similar widths for the Br 4p block (≈ 5 eV in CSC-EH-TB, ≈ 4 eV in TB-LMTO-ASA). Also, the slightly too narrow (see below) band gaps (≈ 2.1 eV in CSC-EH-TB, ≈ 1.5 eV in TB-LMTO-ASA) and the width of the unoccupied Zr "t_{2g}" band region (≈ 0.8 eV in both methods) are about the same.

(16) Abriel, W. *Mater. Res. Bull.* **1982**, *17*, 1341–1346; **1983**, *18*, 1419–1423; **1984**, *19*, 313–318.

(17) Abrahams, S. C.; Ihringer, J.; Marsh, P. *Acta Crystallogr.* **1989**, *B45*, 26–34.

(18) Boysen, H.; Hewat, A. W. *Acta Crystallogr.* **1978**, *B34*, 1412–1418.

(19) Thiele, G.; Mrozek, C.; Kammerer, D.; Wittmann, K. *Z. Naturforsch. B* **1983**, *38*, 905–910.

(20) Van Vleck, J. H. *The Theory of Electric and Magnetic Susceptibilities*; Oxford University Press: Oxford, 1932.

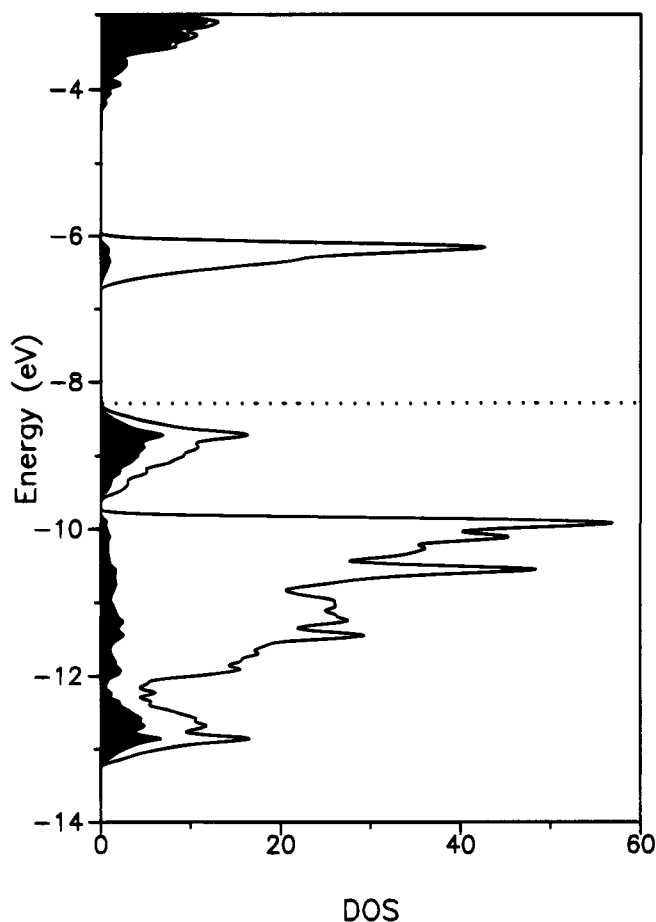


Figure 5. Total and In-projected (black) density-of-states (CSC-EH-TB) for tetragonal In_2ZrBr_6 . The horizontal dashed line is the Fermi level. Indium contributions below -8 eV (Br 4p block) are almost completely 5s in character whereas In 5p begins to mix in above -4 eV.

Just above the Br 4p centered energy range (Figure 5), where the metal contribution is dominated by In 5s functions, there are unoccupied, almost degenerate Zr 4d bands ($l = 2$). They are built up from the d_{xy} , d_{yz} , and d_{xz} wave functions (corresponding to the cubic "t_{2g}" set).²¹ These bands could in principle lead to the observed, almost temperature-independent paramagnetism, provided that there is an interaction with the highest occupied bands just below the Fermi edge (practically pure In 5s, $l = 0$). In other words, a TIP would require that there are nonvanishing transition matrix elements $\langle \phi_1 || \phi_2 \rangle$ between bands below (ϕ_1 , In 5s centered) and above (ϕ_2 , Zr 4d centered) the Fermi level, reflecting their greater-than-zero overlap. Can there be such an electronic coupling?

Two statements should be made here, one which is essentially crystal-chemical and the other one which is more technical, based on theoretical solid state physics. First, the $\text{In}^+ - \text{Zr}^{4+}$ distance (457 pm), more than twice the sum of the ionic radii, is definitely too large for the assumption of a *direct* interaction. Second, the quantitative treatment of van Vleck-type magnetism is very difficult, and only atomic (for example low-spin Co^{3+}) and complex-ion species (MnO_4^- for instance) have been treated by (approximate) computational methods,²² reaching a fair

(21) The wave functions of the "e_g" set are approximately 9 eV apart, at about 2.5 eV one-particle energy. This large splitting is due to the very short $\text{Zr}^{4+} - \text{Br}^-$ distances.

(22) A few examples may be found in the following: *Theory and Applications of Molecular Diamagnetism*; Mulay, L. N., Boudreaux, E. A., Eds.; John Wiley & Sons: New York, London, Sydney, Toronto, 1976. See also: Carlin, R. L. *Magnetochemistry*; Springer: Berlin, Heidelberg, New York, Tokyo, 1986.

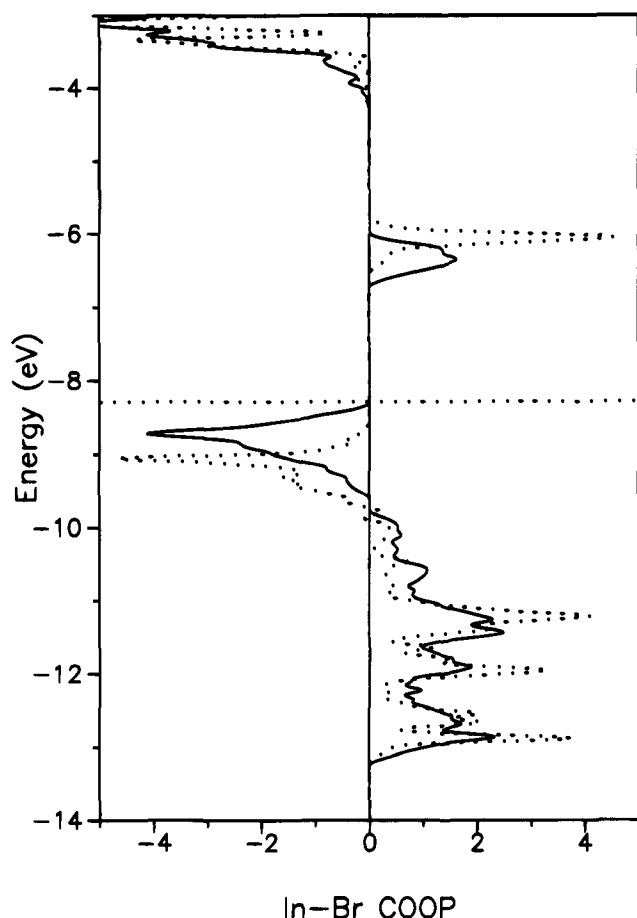


Figure 6. Crystal orbital overlap populations (CSC-EH-TB) for In^+-Br^- interactions in tetragonal In_2ZrBr_6 (solid line) and in the cubically averaged structural description (dotted), respectively. The horizontal dotted line indicates the Fermi energy for tetragonal In_2ZrBr_6 .

quantitative agreement with experiment. At present time, a corresponding *quantitative* understanding of a solid seems to be out of the question not only because the one-electron bands are probably too inaccurate an approximation for setting up the true state wave functions. The computational difficulty is evidently reflected by the failure in calculating the band gaps; they are too small by at least 1–1.5 eV since the slightly greenish-yellow color of the material suggests a band gap of at least 3 eV. While this would be a quite typical TIP energy gap, large compared to kT , none of the two methods is able to reproduce it quantitatively, simply due to the insufficient description of electronic correlation.

However, there is *qualitative* support available for a coupling of the two wave functions (In 5s and Zr “ t_{2g} ”) via bridging Br^- anions, as can be seen from Figure 6. Depicted are the crystal orbital overlap populations of the In^+-Br^- bonds both for the tetragonal real structure (solid line) as well as for the cubically averaged structure (dotted). The chemical bonding will be discussed first:

As found in all other known In^+-Br^- interactions,⁵ there are both bonding (below -10 eV) and antibonding regions (above), a consequence of the (almost) doubly filled In 5s orbital and the reason for the low chemical stability of all these reduced compounds. The integrated overlap population of the In^+-Br^- bonds is $+0.047$ both for the tetragonal real structure and for the cubically averaged one—thus, the symmetry reduction is *not* due to an influence of the InBr_{12}^{11-} unit. A partitioning of the total energy into atomic contributions²³ shows that it is

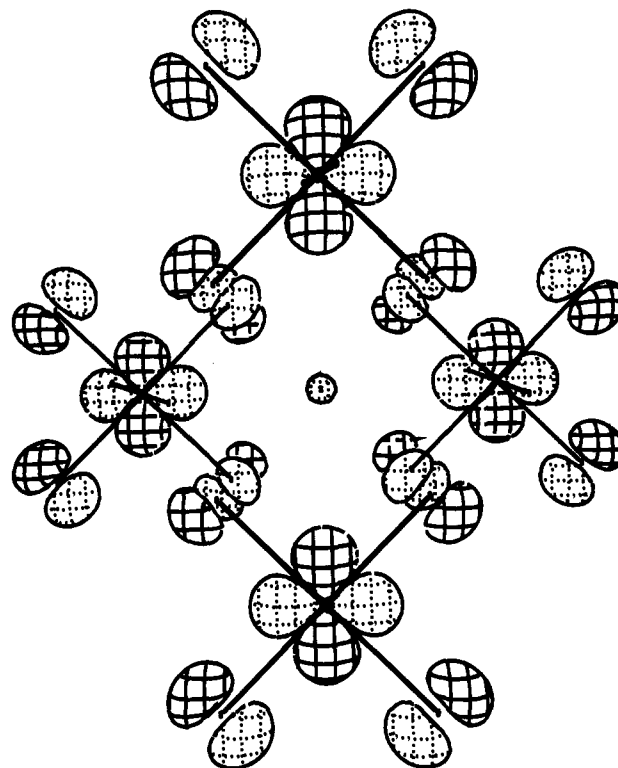


Figure 7. LUMO (at around -6.5 eV) of an $\text{In}^+(\text{ZrBr}_6^{2-})_4$ molecular anion (according to a cut from the structure of tetragonal In_2ZrBr_6) along [001]. The surface value of the wave function is 0.030. In order to obtain a clearer picture and understanding, atomic contributions have been contracted by a factor of 1.5.

mostly the Br^- positions that become energetically stabilized within the tetragonal phase. This is more or less in harmony with classical, electrostatic ways of interpretation. The reduced absolute electronic hardness of tetragonal In_2ZrBr_6 , on the other hand, goes back to the more heterogeneous In^+-Br^- bond distance *spectrum*; the In 5s part shows a slightly larger dispersion and thus is also shifted to regions of higher energy, narrowing the band gap.

The greater-than-zero mixing between the highest occupied, In centered 5s bands and the empty Zr 4d bands (“ t_{2g} ” set) manifests itself in the In^+-Br^- bonding interaction at -6.5 eV (lowest unoccupied crystal orbital = LUCO, Figure 6); it appears at the same energy as the just shown Zr “ t_{2g} ” contribution within the density-of-states curve (Figure 5). The shape of the underlying wave function²⁴ may be approximated by a semiempirical molecular orbital calculation on an In^+ cation that is tetrahedrally coordinated by ZrBr_6^{2-} octahedra exactly like it is within the extended crystal: Figure 7 reveals one of the three (per Zr atom) degenerate LUMOs that, due to the just mentioned indirect coupling, exhibits a little In 5s contribution in addition to mainly Zr 4d and Br 4p character. This small contribution is equally recognizable from the local density-of-states (In projection in black) in the LUCO (Figure 5). To the best of our knowledge, this is the first observation and (at least qualitative) description of an indirectly ($\text{In}^+-\text{Br}^--\text{Zr}^{4+}$) generated paramagnetism according to van Vleck’s theory. One would expect it to show a slight increase in magnitude upon cooling because of slowing down the atomic vibrations of the mediating Br^- anions such that the time average of the $\text{In}^+-\text{Br}^--\text{Zr}^{4+}$ coupling is maximized—this is exactly what can be seen in the molar susceptibility–temperature plot depicted in Figure 4.

(23) Dronskowski, R. *J. Am. Chem. Soc.* **1992**, *114*, 7230–7244.

(24) Program CACAO: Mealli, C.; Proserpio, D. M. *J. Chem. Educ.* **1990**, *67*, 399–402.

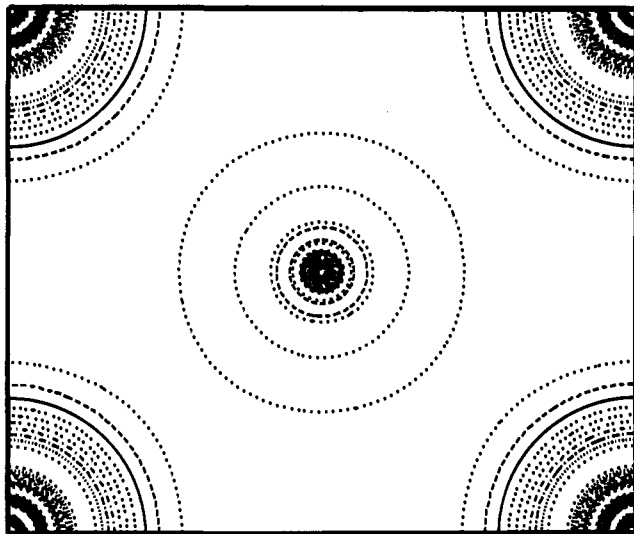


Figure 8. Calculated *ab initio* charge density (TB-LMTO-ASA in full potential mode) within the most compact In^+/Br^- plane (bond distance 350.5(3) pm) of tetragonal In_2ZrBr_6 . The observable quantity is divided into 20 equidistant steps between 0 and $0.35 e/a_0^3$ (a_0 is the Bohr radius of about 52.9 pm). The outermost “ring” around In^+ (center) is $0.0175 e/a_0^3$.

Because of the small size of the here found effect, any predictions as to the expected change in TIP magnitude upon chemical substitutions (Tl against In, other halides against Br) are almost impossible to make. It seems, however, that the most interesting substitution would be a replacement of Zr^{4+} against Th^{4+} , the latter ion having a similar size but a much more complex electronic configuration due to the energetically almost degenerate 6d and 5f atomic orbitals. Corresponding syntheses to yield In_2ThBr_6 are under way.

3.2. Crystal Potential. It is possible to graphically demonstrate the above-mentioned weak bonding of In^+ to its coordinating Br^- neighbors. Figure 8 shows the theoretical charge density within the most compact In^+/Br^- plane in In_2ZrBr_6 , from one of the most reliable *ab initio* methods available for solids at the present time.²⁵ Using a direct comparison between the Br^- (corners) and In^+ (center), the strikingly slow

(25) It is based on non-spin-polarized, scalar-relativistic, self-consistent band structure calculations according to *linear muffin-tin orbital* theory (LMTO)^{34,35} in its tight binding representation.^{36,37} The many-particle picture was obtained through the local density approximation as parametrized by von Barth and Hedin,³⁸ whereas the division of the atomic potentials was done in the framework of the *atomic spheres approximation* (ASA), including a combined correction term. Diagonalization and integration in k space were performed with an improved³⁹ tetrahedron method⁴⁰ at 30 irreducible points and 355 inequivalent tetrahedra. After having reached self-consistency, all simplifying shape approximations for the atomic potentials were dropped in the last step.

decay of the charge density around the cation while moving away from the nucleus is conspicuous, and it reflects a very “soft” crystal potential that acts on In^+ . Within this context, it may be worthwhile remembering that *all* related crystal structure refinements show significantly enlarged displacement parameters for In^+ positions, even when these are fully occupied. It may well be the case that In^+ is subject to “trembling motions” around the “equilibrium position” even at very low temperature, very much in the spirit of a second-order Jahn–Teller instability that has been suggested from the theoretical point of view.⁵ Using *ab initio* methodology, we are calculating the corresponding energy hyper-surface of the tetragonal compound at the present time in order to fully elucidate the phenomenon found here.

Acknowledgment. I am indebted to Dr. Horst Borrmann, Willi Röhrenbach, and Frieder Kögel for their help in the crystallographic studies, to Eva Brücher and Dr. Reinhard K. Kremer for doing the susceptibility measurements, and to Dr. Georges Krier for his expert help in solving programming problems. I would also like to thank Prof. Dr. Arndt Simon for generously supporting my research efforts.

JA9427008

(26) Program for Rietveld Analysis of X-Ray and Neutron Powder Diffraction Patterns: DBW 9006 (rel. 8.4.91); School of Physics (R. A. Young), Georgia Institute of Technology, Atlanta, GA 30322.

(27) McGlynn, S. P.; Vanquickenborne, L. G.; Kinoshita, M.; Carroll, D. G. *Introduction to Applied Quantum Chemistry*; Holt, Rinehart and Winston: New York, 1972.

(28) Hoffmann, R. *J. Chem. Phys.* **1963**, *39*, 1397–1412.

(29) Ammeter, J. H.; Bürgi, H.-B.; Thibeault, J. C.; Hoffmann, R. *J. Am. Chem. Soc.* **1978**, *100*, 3686–3692.

(30) Fitzpatrick, N. J.; Murphy, G. H. *Inorg. Chim. Acta* **1984**, *87*, 41–46; **1986**, *111*, 139–140.

(31) Munita, R.; Letelier, J. R. *Theoret. Chim. Acta (Berlin)* **1981**, *58*, 167–171.

(32) Häussermann, U.; Nesper, R. ETH Zürich (Switzerland); unpublished.

(33) QCPE program EHMACC: Whangbo, M.-H.; Evain, M.; Hughbanks, T.; Kertesz, M.; Wijeyesekera, S.; Wilker, C.; Zheng, C.; Hoffmann, R.

(34) Andersen, O. K. *Phys. Rev. B* **1975**, *12*, 3060–3083.

(35) Skriver, H. L. *The LMTO Method*; Springer: Berlin, Heidelberg, New York, 1984.

(36) Andersen, O. K.; Jepsen, O. *Phys. Rev. Lett.* **1984**, *53*, 2571–2574.

(37) Program TB-LMTO 4.4: van Schilfgaarde, M.; Paxton, T. A.; Jepsen, O.; Andersen, O. K.

(38) von Barth, U.; Hedin, L. *J. Phys. C* **1972**, *5*, 1629–1642.

(39) Blöchl, P. Dissertation, Universität Stuttgart, Germany, 1989.

(40) Jepsen, O.; Andersen, O. K. *Solid State Commun.* **1971**, *9*, 1763–1767.

(41) Increments for Zr^{4+} and Br^- : Selwood, P. W. *Magnetochemistry*, 2nd ed.; Interscience Publishers: New York, 1956. Increment for In^+ (-23×10^{-6} emu/mol): Dronskowski, R. Dissertation, Universität Stuttgart, Germany, 1990.